Available online at www.sciencedirect.com
SCIENCE DIRECT
Thermochimica Acta 438 (2005) 144–154
thermochimica acta
www.elsevier.com/locate/tca

Cationic copolymerization of cycloaliphatic epoxy resin with an spirobislactone with lanthanum triflate as initiator Kinetics of the curing process

Xavier Fernandez, Xavier Ramis, Josep M. Salla *

Laboratori de Termodinàmica, ETSEIB, Universitat Politècnica de Catalunya, Diagonal 647, 08028 Barcelona, Spain

Received 9 May 2005; received in revised form 26 July 2005; accepted 26 July 2005
Available online 30 September 2005

Abstract

3,4-Epoxycyclohexylmethyl 3,4-epoxycyclohexane carboxylate (ECH) was cured with different proportions of 1,6-dioxaspiro[4,4]nonane-2,7-dione (s(γ-BL)) using lanthanum triflate as a catalyst. DSC was used to obtain kinetic data associated to the curing process by means of series of non-isothermal experiments. Fourier transform infrared spectroscopy in attenuated total reflection mode (FT-IR/ATR) was used to study the evolution of the epoxide group in order to compare experimental isothermal data with simulated isothermal data. The complexity of the process itself enabled us to compare different procedures for obtaining isoconversional data and to determine the kinetic model that best describes the curing process.

An increase in the proportion of s(γ-BL) increases the speed of the curing process. By means of applying isoconversional methods to dynamic experimental data, we observed that an increase in the proportion of s(γ-BL) leads to an overall decrease in the activation energy for the different formulations. Kinetic parameters that were determined using both differential and integral isoconversional procedures were compared. This allowed us to analyze and to discuss the usefulness of different methods in order to obtain a suitable kinetic triplet at each step of the curing of the ECH/s(γ-BL) system using lanthanum triflate as a catalyst.

Keywords: Epoxy resin; Lactone; Isoconversional methods; DSC; Kinetic model

1. Introduction

The curing of thermosetting materials is accompanied by some degree of shrinkage, which can lead to internal stress in the material, poor adhesion of coatings to the substrate and the appearance of microvoids and microcracks, which reduce the durability of materials [1–3].

Shrinkage during curing can be reduced by using expanding monomers. Spiroorthoesthers (SOEs) and spiroorthocarbonates (SOCs) are examples of expanding monomers with reduced shrinkage in ring-opening polymerizations [1–3]. SOEs are obtained by the reaction of epoxides with lactones under cationic catalysis [3,4]. However, their high cost limits their use to few technological applications. The copolymerization of epoxy resins with lactones may take place via formation and reaction of intermediate SOE groups, thus reducing shrinkage [1,2,5–7].

DGEBA epoxy resins were successfully copolymerized with γ-butyrolactone using lanthanide triflates as catalysts and a reduction in the shrinkage after gelation [1,2] was observed. The competitive reactions that take place during the curing process were identified. The polymerization of SOEs at the end of the curing process has been reported to be responsible for the reduction in shrinkage [2]. Similar studies have been performed with 3,4-epoxycyclohexylmethyl-3,4-epoxycyclohexanecarboxylate (ECH) and γ-butyrolactone [5]. Both systems show an increase in the reaction rate as the proportion of γ-butyrolactone increases [1,2,5].

Recently, the copolymerization of ECH (Scheme 1, left) and 1,6-dioxaspiro[4,4]nonane-2,7-dione (s(γ-BL), Scheme 1, right) has been studied [7]. A reduction in shrink-

* Corresponding author. Tel.: +34 934016591; fax: +34 934017389.
E-mail address: salla@mmt.upc.edu (J.M. Salla).

0040-6031/$ – see front matter © 2005 Elsevier B.V. All rights reserved.
doi:10.1016/j.tca.2005.07.012

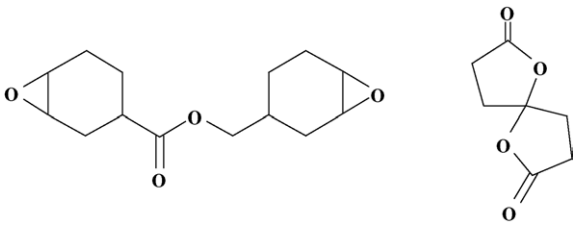

Scheme 1.

age after gelation due to the formation and the reaction of intermediate SOE groups and homopolymerization of s(γ-BL) was observed. From an overall thermal characterization it was observed that the heat released during curing was related to the amount of the epoxide group and remained almost constant for the different formulations. It was found that the formulation with the highest s(γ-BL) content did not react completely.

In this work we investigated the kinetics of the curing process for the ECH/s(γ-BL) system using lanthanum triflate as a catalyst. DSC is used to determine the heat released during curing and to obtain non-isothermal kinetic data from a series of dynamic experiments at different heating rates. The complexity of the process allowed us to analyze the usefulness of different methods in order to obtain a suitable kinetic triplet at each step of the curing process. Integral and differential isoconversional methods were applied to non-isothermal data and the results were compared. A kinetic model giving an approximate description of the curing process was established in agreement with the experimental isoconversional data and model-free calculations. The pre-exponential factor obtained with this procedure together with the activation energy allowed us to compare the different formulations more accurately.

FT-IR was used to monitor the conversion of the epoxide group in isothermal experiments. Simulated isothermal data from the dynamic experiments carried out in the DSC were compared with the experimental isothermal conversion of the epoxide group.

2. Experimental

2.1. Materials

ECH epoxy resin (epoxy equiv. = 126 g/eq) (Araldite CY 179, Vantico) and s(γ-BL) (molecular mass = 156 g/mol, 98%) (Aldrich) were used as received. Lanthanum (III) trifluoromethanesulfonate (99.99%) (Aldrich) was used without purification.

2.2. Preparation of the curing mixtures

Samples were prepared by adding to the corresponding proportions of s(γ-BL) and ECH 1 phr of lanthanum triflate (1 part per 100 parts of mixture, w/w). ECH was kept for a while at room temperature and s(γ-BL) was crushed with a mortar before mixing. Samples were carefully stirred and kept at −18 °C before use to prevent polymerization.

Table 1
Relation between the various formulations studied, notation and proportion of reactants, which contain 1 phr of lanthanum triflate as initiator

Formulation	Notation	Molar ratio ECH:s(γ-BL)	s(γ-BL) (%, w/w)	Mol catalyst/ eq epoxy
ECH/s(γ-BL) 1:0	1:0	1:0	0	0.00215
ECH/s(γ-BL) 6:1	6:1	6:1	9.4	0.00237
ECH/s(γ-BL) 4:1	4:1	4:1	13.4	0.00248
ECH/s(γ-BL) 2:1	2:1	2:1	23.6	0.00282
ECH/s(γ-BL) 1:1	1:1	1:1	38.2	0.00348

Table 1 shows the various formulations that were used, their notation and the proportions of the different reactants.

2.3. DSC calorimetry

The samples were dynamically cured using a Mettler DSC-821e calorimeter with a TSO801RO robotic arm. Samples of approximately 10 mg in weight were cured in aluminium capsules in a nitrogen atmosphere. Dynamic experiments were performed between 0 and 200 °C at heating rates ranging from 2 to 15 °C/min to determine the reaction heat and to obtain kinetic data.

The degree of conversion α and the reaction rate $d\alpha/dt$ in dynamic curing processes were calculated as follows:

$$\alpha = \frac{\Delta H_T}{\Delta H_{dyn}}, \qquad \frac{d\alpha}{dt} = \frac{(dH/dt)}{\Delta H_{dyn}} \tag{1}$$

where ΔH_{dyn} is the total heat released during the curing process, ΔH_T is the heat released up to a temperature T and dH/dt is the instant heat released.

In isothermal processes, the degree of conversion may be obtained directly from isothermal experiments or indirectly by means of the residual heat released during dynamic post-curing after isothermal curing:

$$\alpha = 1 - \frac{(\Delta H_{res})_t}{\Delta H_{dyn}} \tag{2}$$

where $(\Delta H_{res})_t$ is the residual heat after an isothermal curing up to a time t.

2.4. FT-IR spectroscopy

Samples were cured isothermally at 100, 110 and 120 °C in a FT-IR Bomem Michelson MB 100 spectrophotometer, with a resolution of 4 cm^{-1} in the absorbance mode. An attenuated total reflection accessory with thermal control and a diamond crystal (Golden Gate Heated Single Reflection Diamond ATR, Specac-Teknokroma) was used in order to determine the FT-IR spectra.

The disappearance of the absorbance peak at 795 cm^{-1} (oxirane ring deformation) was used to monitor the epoxy conversion. The increase in the absorbance peak at

1075 cm^{-1} (C–O–C stretching of linear aliphatic ether), which was not used for further calculations, showed that epoxy homopolymerization took place. The peak at 1450 cm^{-1} (methylene group) was chosen as an internal standard. Thus, the normalized absorbances were calculated as follows:

$$A^*_{xxx} = \frac{A_{xxx}}{A_{1450}} \tag{3}$$

The conversion of the epoxide was determined by the Lambert–Beer law from the normalized changes of absorbance at 795 cm^{-1}, as

$$\alpha_{\text{epoxy}} = 1 - \left(\frac{A^*_{795,t}}{A^*_{795,0}}\right) \tag{4}$$

where $A^*_{795,t}$ is the normalized absorbance corresponding to the peak at 795 cm^{-1} at a given time t and $A^*_{795,0}$ is the normalized absorbance at the beginning of the curing process.

3. Theoretical analysis

3.1. Determination of kinetic parameters using isoconversional methods

In reaction processes in a condensed phase, it is usually accepted that the reaction rate is given by

$$\frac{d\alpha}{dt} = kf(\alpha) = A\exp\left(\frac{-E}{RT}\right) f(\alpha) \tag{5}$$

where k is the kinetic constant, A and E are the pre-exponential factor and the activation energy for the reaction according to the Arrhenius equation for the kinetic constant k, R is the universal gas constant, T is the temperature and $f(\alpha)$ is a function that depends on the degree of conversion and represents the kinetic model that governs the process.

This equation can be expressed in its integral form as follows:

$$g(\alpha) = \int_0^\alpha \frac{d\alpha}{f(\alpha)} = \int_0^t A\exp\left(-\frac{E}{RT}\right) dt \tag{6}$$

Isoconversional methodology assumes that, at a given degree of conversion, the reaction mechanism does not depend on the temperature of reaction in isothermal experiments or on the heating rate in dynamic experiments. Therefore, each degree of conversion α will have its corresponding activation energy E_α, a frequency factor A_α and a kinetic model resulting from differential $f(\alpha)$ or integral $g(\alpha)$ functions.

By applying logarithms to Eq. (5), the following expression is obtained, which is the basis of the differential or Friedman [8] method for obtaining kinetic data.

$$\ln\left(\frac{d\alpha}{dt}\right)_\alpha = \ln(A_\alpha f(\alpha)) - \frac{E_\alpha}{RT_\alpha} \tag{7}$$

Based on this equation and establishing a correlation between $\ln(d\alpha/dt)_\alpha$ and $1/T_\alpha$, the activation energy E_α and the parameter $A_\alpha f(\alpha)$ are obtained, both for isothermal and dynamic experiments.

In isothermal processes Eq. (6) can be integrated and reorganized as:

$$\ln t_\alpha = \ln\left(\frac{g(\alpha)}{A_\alpha}\right) + \frac{E_\alpha}{RT_\alpha} \tag{8}$$

As it can be seen, activation energy E_α and pre-exponential factor A_α are supposed to be constant up to a degree of conversion α. Kinetic parameters are obtained in a very similar way to the differential method by correlating $\ln t_\alpha$ with $1/T_\alpha$ for different isothermal experiments.

For dynamic experiments, at the constant heating rate $\beta = dT/dt$, Eq. (6) is expressed as follows:

$$g(\alpha) = \frac{A_\alpha}{\beta}\int_0^{T_\alpha} \exp\left(-\frac{E_\alpha}{RT}\right) dT \tag{9}$$

Integral (9) does not have an analytical solution and we can therefore estimate its solution, based on

$$\frac{A_\alpha}{\beta}\int_0^{T_\alpha} \exp\left(-\frac{E_\alpha}{RT}\right) dT = \frac{A_\alpha}{\beta} I(E_\alpha, T_\alpha) \tag{10}$$

$$I(E_\alpha, T_\alpha) = \frac{E_\alpha}{R} p(x) \tag{11}$$

where $p(x)$ is a function of $x = E_\alpha/RT_\alpha$, which enables us to estimate the solution of the integral with a certain error rate.

There are simplified expressions of $p(x)$ that enable us to obtain linear expressions comparable to Eqs. (7) and (8). These include the equations deduced by Doyle [9], on which the Flynn–Wall–Ozawa [10] integral isoconversional method is based (Eq. (12)), and deduced by Murray and White [11] and Coats–Redfern [12], which is the basis for the Kissinger–Akahira–Sunose integral isoconversional method [13,14] (Eq. (13)).

$$\log\beta = \log\left[\frac{A_\alpha E_\alpha}{g(\alpha)R}\right] - 2.315 - 0.4567\frac{E_\alpha}{RT_\alpha} \tag{12}$$

$$\ln\left(\frac{\beta}{T_\alpha^2}\right) = \ln\left[\frac{A_\alpha R}{g(\alpha)E_\alpha}\right] - \frac{E_\alpha}{RT_\alpha} \tag{13}$$

Starink [15] proposes that equations of the type $p(x) = \exp(-Ax + B)/x^k$ applied to Eqs. (10) and (11) give rise to direct methods, from which it is possible to obtain the activation energy for the linearization of experimental data. By choosing the appropriate A, B and k parameters it is possible to obtain expressions (12) and (13).

The great advantage of these linear models is that isoconversional data can be obtained without the need for complex calculations. The error rate in some of these equations varies according to the range of experimental data and can be large depending on the value of x, although it can be reduced by choosing the appropriate values for A, B and k.

There are other more complex variations of $p(x)$, such as those advanced by Senum and Yang [16] or Agrawal [17],

whose approximations of the temperature integral at an interval of x offer a far higher degree of accuracy and a lower error rate, but which do not allow results to be obtained so directly.

Vyazovkin proposes a different mathematical development for obtaining integral isoconversional data without needing to use linear solutions, which is applicable to any temperature profile [18]. The original method, for constant heating rates, uses Senum and Yang's third-order approximation, which gives an error rate of less than 0.02%, even when $x = 5$ [16,19,20]:

$$p(x) = \frac{e^{-x}}{x}\frac{x^2 + 10x + 18}{x^3 + 12x^2 + 36x + 24} \tag{14}$$

In the light of a series of dynamic experiments with varying heating rates, the following requirement must be met:

$$\frac{A_\alpha}{\beta_1} I(E_\alpha, T_{\alpha,1}) = \cdots = \frac{A_\alpha}{\beta_n} I(E_\alpha, T_{\alpha,n}) \tag{15}$$

The activation energy for a given conversion is obtained by finding the minimum of the function

$$\phi(E_\alpha) = \sum_{i}^{n}\sum_{j\neq i}^{n} \frac{I_i(E_\alpha, T_{\alpha,i})/\beta_i}{I_j(E_\alpha, T_{\alpha,j})/\beta_j} \tag{16}$$

The problem with all integral methods is that they impose a constant activation energy and pre-exponential factor from 0 conversion to α as a solution of the integral in Eq. (9), and therefore different to the instantaneous activation energy that can be obtained from differential data [21]. This is also true of the integral method given in Eq. (8), where the isothermal conditions do not make any additional mathematical development necessary and no error occurs in the solution of the temperature integral; however, it does assume a constant activation energy and pre-exponential factor.

Vyazovkin proposes a modification in his method [21], by which an instantaneous activation energy is obtained from integral data. This modification, adapted to experiments with a constant heating rate, is expressed as follows:

$$\begin{aligned} g(\alpha) - g(\alpha - \Delta\alpha) &= \int_{\alpha-\Delta\alpha}^{\alpha} \frac{d\alpha}{f(\alpha)} = \frac{A_\alpha}{\beta}\int_{T_{\alpha-\Delta\alpha}}^{T_\alpha} \exp\left(-\frac{E_\alpha}{RT}\right) dT \\ &= \frac{A_\alpha}{\beta} J(E_\alpha, T_\alpha) \end{aligned} \tag{17}$$

In order to find the instantaneous activation energy, as was the case above, the minimum of the function must be found:

$$\phi(E_\alpha) = \sum_{i}^{n}\sum_{j\neq i}^{n} \frac{J_i(E_\alpha, T_{\alpha,i})/\beta_i}{J_j(E_\alpha, T_{\alpha,j})/\beta_j} \tag{18}$$

The integral $J(E_\alpha,T_\alpha)$ can be solved by a numerical integration in the temperature range $T_{\alpha-\Delta\alpha} - T_\alpha$, or by approximating

$$J(E_\alpha, T_\alpha) = I(E_\alpha, T_\alpha) - I(E_\alpha, T_{\alpha-\Delta\alpha}) \tag{19}$$

using, as above, Senum and Yang's approximation for solving both integrals more rapidly.

The lower the value of $\Delta\alpha$, the lower the error rate, as the interval in which the activation energy is assumed to be constant is smaller. Thus, with an appropriate $\Delta\alpha$ value, activation energy values can be obtained that are very similar to those that would be obtained with Eq. (7).

Hereinafter, Vyazovkin's original method and his modification will be known as integral and modified integral, respectively.

3.2. Determining the kinetic model

By means of isoconversional procedures, the activation energy E_α can be obtained, which is associated with each degree of conversion, but the pre-exponential factor A_α and the kinetic model (functions $f(\alpha)$ or $g(\alpha)$) cannot be obtained separately. Once the kinetic model is known, the determination of the pre-exponential factor is immediate.

Various methods for determining the kinetic model were used, both for differential and integral data. One such method is the Coats–Redfern method [12] for dynamic integral data, as expressed in the following equation:

$$\ln\left(\frac{g(\alpha)}{T^2}\right) = \ln\left[\frac{AR}{\beta E}\right] - \frac{E}{RT} \tag{20}$$

Given the heating rate β, the temperature profile in relation to the conversion and the kinetic model $g(\alpha)$, the representation of $\ln(g(\alpha)/T^2)$ in relation to $1/T$ enables us to determine the average activation energy E and average pre-exponential factor A for the entire experiment. The model with the best correlation coefficient is chosen along with an activation energy similar to that obtained isoconversionally.

With differential data, we can use Eq. (7) reorganized as follows:

$$\ln\left(\frac{d\alpha/dt}{f(\alpha)}\right) = \ln A - \frac{E}{RT} \tag{21}$$

In this case, the kinetic model $f(\alpha)$, the reaction rate $(d\alpha/dt)$ and the temperature profile in relation to the conversion are needed. By means of the correlation of $\ln((d\alpha/dt)/f(\alpha))$ versus $1/T$, an average activation energy E and an average pre-exponential factor A are obtained, in a similar way that those obtained by the Coats–Redfern method. Likewise, an activation energy value that is similar to that obtained isoconversionally and a high correlation coefficient are sought.

The activation energy and the pre-exponential factor may be linked due to the compensation effect or the isokinetic relationship [1,22,23] in the following way

$$\ln A_\xi = a + bE_\xi \tag{22}$$

where ξ can be any of the factors that bring about an alteration in the activation energy values and in the frequency factor. This equation is a natural derivation of the Arrhenius equation for the kinetic constant, $\ln k = \ln A - E/RT$. The parameter a is therefore associated with an isokinetic constant, $a = \ln k_{iso}$,

and the parameter b is related to an isokinetic temperature, where $b = (RT_{iso})^{-1}$.

In multi-step processes, the activation energy may vary according to the degree of conversion due to existence of reactions with different activation energies. The overall activation energy may vary throughout the process as the temperature changes, thus giving rise to an isokinetic relationship. According to certain authors [22], the isokinetic temperature associated with this isokinetic relationship can take on an arbitrary value within the range of experimental data, but only when the kinetic model corresponds to that which governs the process.

The compensation effect in relation to the conversion can be applied to both integral and differential data. Based on the isoconversional data, the model $g(\alpha)$ or $f(\alpha)$ is used, the factor A_α is calculated and correlated with E_α. The valid model will be that which gives off an isokinetic temperature within the experimental range, with a reasonable correlation coefficient.

Other factors that can bring about an isokinetic relationship are the heating rate and the kinetic model [22,23]. By using the activation energies and the average pre-exponential factors for each model, obtained by means of the Coats–Redfern integral method, or using Eq. (20) for the differential data, a compensation effect can be established in relation to the kinetic model [22].

Vyazovkin proposes that the real pre-exponential factor can be predicted by using the isoconversional activation energies and the compensation effect in relation to the kinetic model, at an average heating rate, without needing to know the kinetic model [22]. In order to determine the most appropriate kinetic model, the existing deviation between the predicted value of $\ln A_\alpha$ can be calculated from the compensation in relation to the kinetic model and that obtained by applying the model $f(\alpha)$ or $g(\alpha)$ to the isoconversional data as

$$\text{error}\,(\%) = 100 \times \frac{1}{n}\sum_{\alpha}\frac{|\ln A_{\alpha,\text{pred}} - \ln A_{\alpha,\text{iso}}|}{\ln A_{\alpha,\text{pred}}} \tag{23}$$

where n represents the number of elements on which the error rate is calculated (for example, a 0.1–0.9 conversion, with $\Delta\alpha$ of 0.01 resulting in $n = 81$), $\ln A_{\alpha,\text{pred}}$ is the predicted factor based on the compensation in relation to the model and $\ln A_{\alpha,\text{iso}}$ is the factor calculated by applying the model to the isoconversional data. The most suitable model is that which presents the lowest error or deviation rate.

There are other methods for determining the kinetic model, such as the Criado method or master curves [24]. Based on the representation of $z(\alpha)/z(0.5)$, where $z(\alpha) = f(\alpha)g(\alpha)$, a model can be determined graphically. The value of $z(\alpha)/z(0.5)$ for experimental data can be calculated as follows:

$$\frac{z(\alpha)}{z(0.5)} = \frac{f(\alpha)g(\alpha)}{f(0.5)g(0.5)} = \left(\frac{T_\alpha}{T_{0.5}}\right)^2 \frac{(\mathrm{d}\alpha/\mathrm{d}t)_\alpha}{(\mathrm{d}\alpha/\mathrm{d}t)_{0.5}} \tag{24}$$

This procedure assumes a constant activation energy throughout the reaction. Therefore, the integral and differential data are constant and equal, and the simplified Eq. (24) can be obtained from Eqs. (5) and (9). If this is not true, or if there is too great a difference between the differential and integral energies, an accurate result cannot be guaranteed by using this method.

Some of these methods have been used in different experiments with consistent results [1,23,25,26].

3.3. Simulation of dynamic and isothermal experiments

Both dynamic and isothermal simulation experiments can be carried out without needing to know the kinetic model.

From the integral methods the parameters E_α and $A_\alpha/g(\alpha)$ are obtained. By using the same equations that were used to obtain these parameters, it is possible to simulate dynamic experiments accurately by finding the temperature corresponding to each degree of conversion at a given heating rate. Whatever the case, it is important not to mix the data obtained by one method for simulation experiments by using the equation of the other method, as different approximations are used to solve the temperature integral.

Isothermal experiments can be simulated based on Eq. (8), using the data obtained from the integral methods. By introducing E_α and $A_\alpha/g(\alpha)$ to Eq. (8), we can determine the time associated with each degree of conversion at a given reaction temperature.

Based on differential data, both the dynamic and isothermal reaction rate curves can be found using Eq. (5), if the parameters E_α and $A_\alpha f(\alpha)$ are known, by applying a constant temperature or any other temperature profile. For the simulation of conversion curves, numerical integration of Eq. (5) is performed using the isoconversional data.

4. Results and discussion

4.1. DSC kinetic analysis using isoconversional methods

Dynamic experiments with DSC at 2, 5, 10 and 15 K/min for each of the formulations were carried out. Figs. 1 and 2 show the reaction rate and conversion curves in relation to temperature for the various formulations at 5 K/min, respectively.

Firstly, it can be seen how the increase in the s(γ-BL) proportion in the formulations accelerates the reaction process, resulting in increasingly lower temperatures for the same conversion. There are no significant changes when the conversion curves for formulations 4:1 and 2:1 are compared. However, changes in the reaction rate curves can be observed, which would lead one to think that a change in the reaction process takes place due to the presence of the s(γ-BL). We have already discussed the difference between the two reaction processes [7].

In the set of reaction rate curves a very significant change can be observed in formulation 1:1, due to its high proportion of s(γ-BL). In a previous paper [7], a general characterization

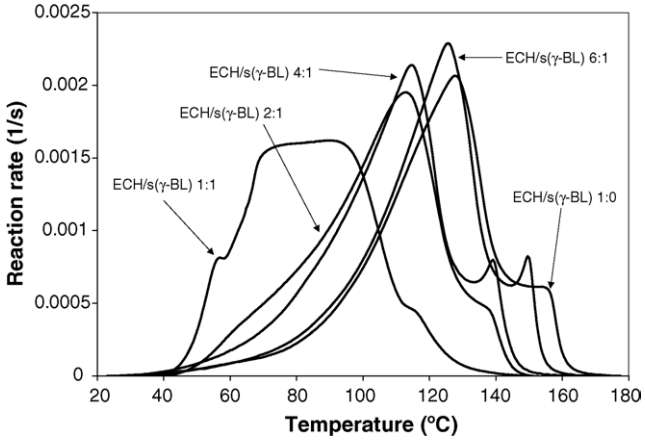

Fig. 1. Reaction rate in relation to temperature, for the various formulations, at 5 K/min.

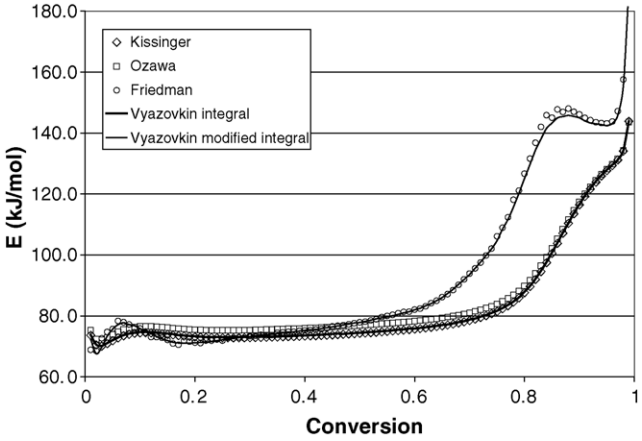

Fig. 3. Representation of activation energy in relation to the conversion for formulation 1:0, obtained based on the integral methods of Kissinger–Akahira–Sunose, Flynn–Wall–Ozawa and Friedman, and on Vyazovkin's integral and modified integral methods.

of the various formulations was carried out, and it was seen that the system had not reacted completely for formulation 1:1.

Throughout the reaction process the activation energies were found by applying isoconversional methods to experimental data. On the one hand, the integral methods given by Eqs. (12) and (13) were used, and on the other hand, the differential method (Eq. (7)) was used.

By way of comparison, we also used the Vyazovkin integral method for experiments at a constant heating rate (Eqs. (10), (11) and (14)–(16)), which gave results comparable to conventional integral methods, and in its modified version (Eqs. (17)–(19)), which gave similar results to the Friedman method. The two methods were applied by making $\Delta\alpha$ equal to 0.01. As the Vyazovkin integral method uses Senum and Yang's approximation as an integral temperature solution, which has a wider range of validity, it will serve to determine which of the other integral approximations given by Eqs. (12) and (13) is the most accurate.

Fig. 3 shows the activation energies obtained from formulation 1:0 using Eqs. (12) and (13), the Friedman method and both integral and modified integral Vyazovkin methods. On the one hand, it can be seen that Vyazovkin's modified integral method is an accurate approximation of the data obtained from the Friedman method. Given that Friedman method gives directly the $Af(\alpha)$ parameter, which can be used for further calculations, we choose the Friedman method.

On the other hand, it can be seen that for the experimental data as a whole, Vyazovkin's integral method gives results that are closer to Eq. (13) than to Eq. (12). Therefore, the data obtained for Eq. (13) will be taken as accurate for simulating other processes with integral data.

With the data obtained from Eqs. (12) and (13), dynamic experiments were simulated, as has been explained in previous sections. Fig. 4 shows the simulation of dynamic experiments with the data obtained from Eq. (13). The simulation is an accurate approximation of the experimental data, which is

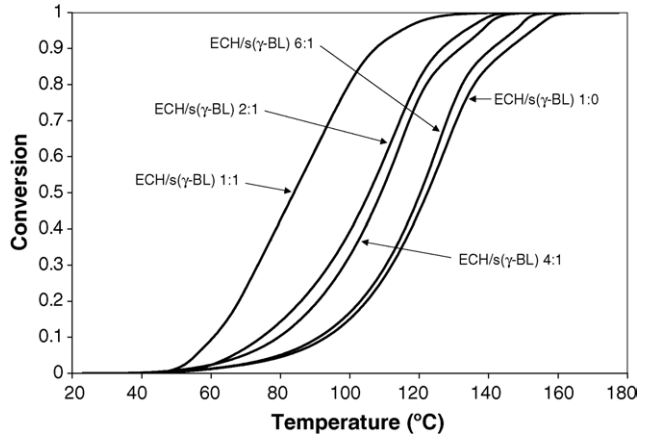

Fig. 2. Conversion in relation to temperature, for the various formulations, at 5 K/min.

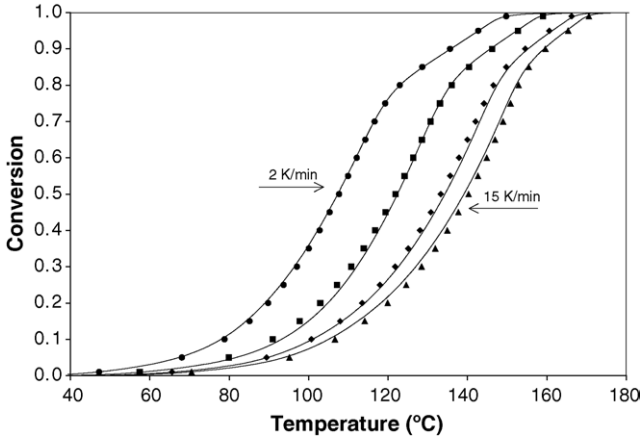

Fig. 4. Simulation of dynamic curing curves for formulation 1:0 based on data obtained using the Kissinger–Akahira–Sunose isoconversional method.

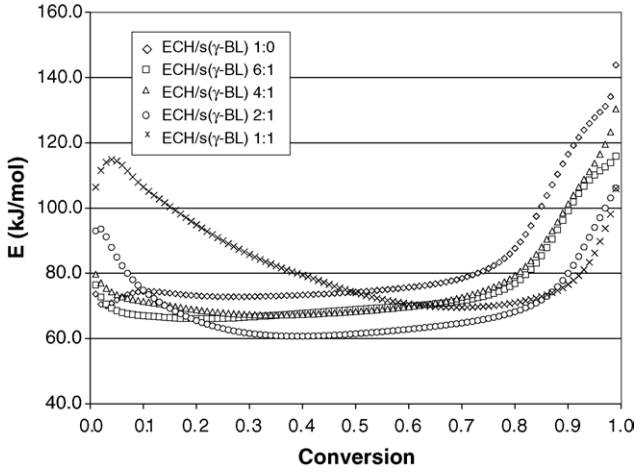

Fig. 5. Activation energy in relation to the conversion for the different formulations, using Kissinger–Akahira–Sunose integral method.

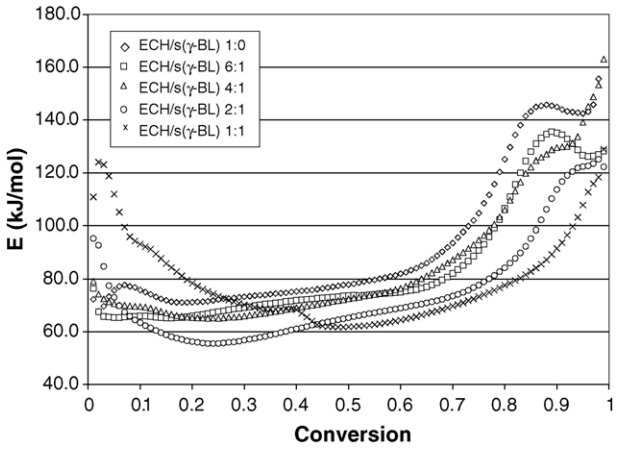

Fig. 6. Activation energy in relation to the conversion for the different formulations, using Vyazovkin's modified integral method.

logical if Eq. (13) was used for the simulation. By using the data obtained from Eq. (12) and using the same equation to simulate the dynamic experiments, the results obtained were just as good. Therefore, in this case, using the equations consistently has more influence on the final result than the error of the integral method used for obtaining isoconversional data when dynamic simulations are carried out. It was seen that by mixing the data from one method with the equation of another to simulate the processes, the results were far different from the experimental behaviour.

Fig. 5 shows a graph of the activation energy in relation to conversion for the various formulations, obtained from Eq. (13). In general, the curves follow the same pattern: a high initial value that decreases due to the reaction's auto-acceleration; a more or less stable value throughout the reaction process; finally, an increase in the value of the activation energy to high conversions, which may be caused by side reactions at the end of the curing process. For the 1:1 formulation, which is the richest in s(γ-BL), the behaviour is quite different. This could already be guessed from Fig. 1, in which the shape of the curve would seem to indicate the presence of numerous reaction processes. By comparing the various formulations, it can be seen that by increasing the proportion of s(γ-BL) in the formulation, the activation energy decreases in the reaction process.

Fig. 6 shows graphs of the activation energies in relation to the conversion for the various formulations obtained from the differential model. The general shape of the curve follows the same pattern as the previous case, but the changes in activation energy are more pronounced.

It must be taken into account that in integral methods each α shows an average value for the activation energy from the start of the reaction until this conversion, whilst differential methods give a value for the activation energy that corresponds to the state of the reaction process in this conversion, as stated in Section 3.1. Therefore, in the integral methods these abrupt changes that are observed in the differential activation energy become less pronounced, which can conceal phenomena that take place in a short conversion interval. There are no drawbacks in simulating a process if one takes into account the different interpretation that the activation energy has in integral methods and in differential methods, and if the equations are not mixed. However, to explain the phenomena that can occur in the reaction process it is better to take the differential data.

Fig. 7 shows superimposed activation energy curves and the rate of reaction to conversion, for the 4:1 formulation. In high conversions, there is a significant increase in the activation energy. In the 1:0 and 6:1 formulations, besides the increase, a maximum relative is observed that can be associated with a second peak that was observed in the dynamic curing of the samples. Several authors [27] have associated the appearance of these peaks at the end of the reaction in the case of the homopolymerization of ECH resin with reactions of transesterification and formation of cycloethers. Even

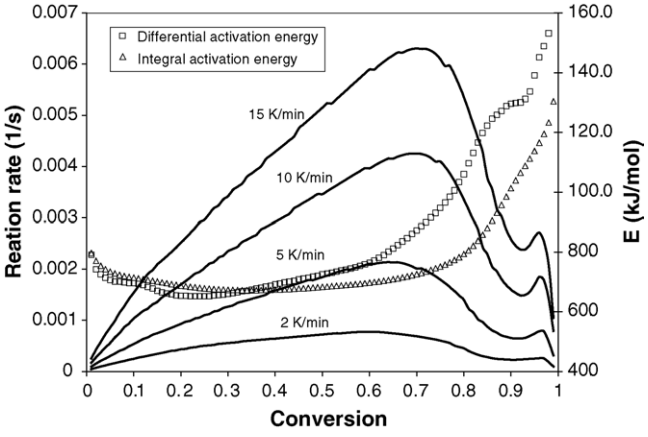

Fig. 7. Integral and differential activation energies obtained, and rate of reaction at different heating rates in relation to the conversion, for formulation 4:1.

though integral methods show a considerable increase in the activation energy for high conversions, they do not show the latter process as clearly.

It was observed through FT-IR, in samples partially cured in DSC, that when the temperature of this second peak is reached the conversion is already high and the amount of the epoxy group cannot be detected in the sample. This peak, therefore, would be associated with secondary reactions that take place once the ECH resin has been exhausted in the formulations. It was seen that the formulations that were richest in ECH had a higher homopolymerization of the ECH resin than other competitive reactions [7]. Therefore, it is also possible that this final process is associated with the amount of homopolymerized ECH resin.

It was therefore observed that the activation energy at the end of the reaction could be associated with the reactions that take place as a consequence of the presence of ECH resin, at high temperatures and once a high degree of curing has been reached.

4.2. FT-IR monitoring of the reactions

FT-IR monitoring of the reactions was carried out at temperatures of 100, 110 and 120 °C. Fig. 8 shows a graph of the conversion of the epoxy group for the 1:0 formulation at different temperatures.

To verify the validity of the dynamic method for obtaining kinetic information about the process, different isotherms were simulated using the isoconversional data obtained from Eq. (13), validated by means of the Vyazovkin integral method, as has already been seen in Section 4.1, and using Eq. (8). In this case, it is important to be consistent when using kinetic data obtained through an integral method with an equation that is also integral, as in both cases the activation energy represents an average value up to a certain degree of conversion.

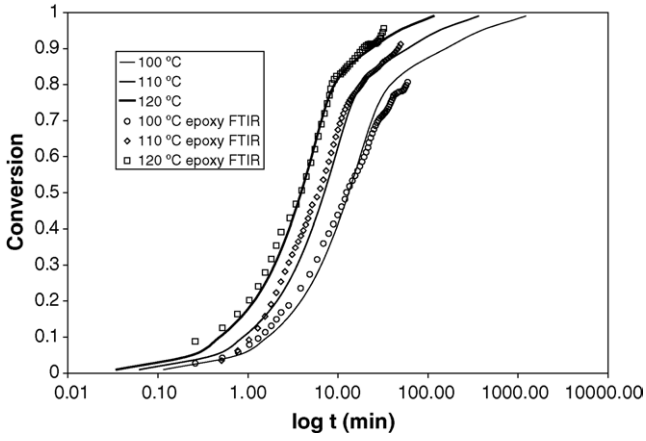

Fig. 8. Conversion in relation to time for formulation 1:0 at different temperatures. Simulated conversion based on calorimetric data are represented by unbroken lines. The symbols represent the conversion of the epoxy group obtained by FT-IR.

Fig. 8 also shows graphs of the simulated isotherms, and it can be seen that the correspondence between the simulation and the experimental data is fairly good. This makes it clear that the kinetic data obtained are valid, and that there is a good rate of correspondence between the thermally calculated conversion and the chemical conversion obtained by FT-IR. Although the integral methods do not give instantaneous activation energy for each conversion, they do serve to simulate curing. We simulated isotherms corresponding to the conversion of the epoxy group using the 4:1 formulation, which were compared to the experimental isotherms with the same degree of success.

4.3. Determining the kinetic model

The kinetic model was determined for the 1:0 and 4:1 formulations using the methods presented in Section 3.2. References [1,25] contain the functions $f(\alpha)$ and $g(\alpha)$ corresponding to the various kinetic models used.

The Criado method assumes that the activation energy and the pre-exponential factor are constant throughout the reaction, which means that the integral and differential data are interchangeable. The application of the Criado method for this system is shown in Fig. 9, where the reduced curves by the 1:0 formulation at different heating rates can be seen. It can be observed that there is almost no correspondence with the curves of the models in conversions above 0.5. As can be seen from the isoconversional data for the different formulations, the activation energy undergoes fairly significant changes during the reaction, which become greater in conversions above 0.5, thus invalidating the Criado method for this system.

The Coats–Redfern method (Eq. (20)) and its differential version (Eq. (21)) were applied. In both cases, a 0.1 a 0.9 conversion interval was used in steps of 0.01. Table 2 shows that the F1 model best reflects the process for both the integral and the differential data. The average activation energy

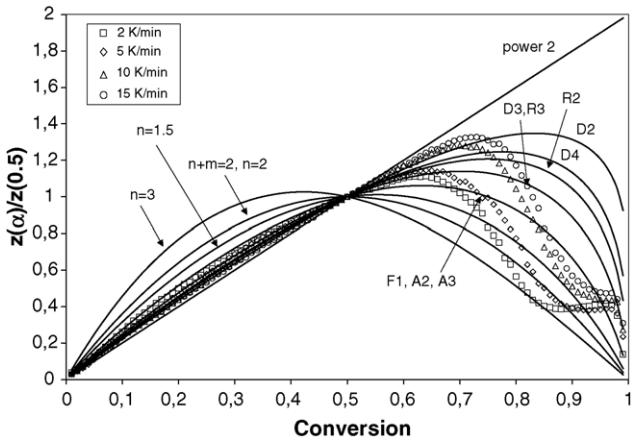

Fig. 9. Criado method for formulation 1:0. Theoretical models are represented by unbroken lines. The symbols represent the experiments at various heating rates.

Table 2
Determining the kinetic model (Eqs. (20) and (21)) and compensation in relation to the kinetic model, for formulation 1:0

Models	Integral data (Eq. (20))						Differential data (Eq. (21))					
	5[a]			10[a]			5[a]			10[a]		
	r^2	E (J/mol)	$\ln A$ ($\min^{-1}$)	r^2	E (J/mol)	$\ln A$ ($\min^{-1}$)	r^2	E (J/mol)	$\ln A$ ($\min^{-1}$)	r^2	E (J/mol)	$\ln A$ ($\min^{-1}$)
D1	0.9745	107290	30.21	0.9923	105695	29.47	0.7228	71787	19.27	0.8769	83548	22.83
D2	0.9853	119900	33.70	0.9974	117825	32.71	0.8619	94496	25.89	0.9505	105284	28.97
D3	0.9941	135723	37.41	0.9990	132956	36.08	0.9480	121890	33.17	0.9861	131383	35.64
D4	0.9890	125112	33.92	0.9985	122811	32.82	0.9011	103947	27.41	0.9684	114281	30.28
F1	0.9973	73096	20.60	0.9957	71246	20.05	0.9349	68713	19.31	0.9785	78669	22.36
R2	0.9895	60711	15.74	0.9988	59418	15.47	0.7122	41798	9.98	0.9063	53016	13.63
R3	0.9933	64603	16.65	0.9989	63141	16.29	0.8222	50770	12.45	0.9478	61567	15.90
A2	0.9967	33289	7.89	0.9950	32286	7.92	0.7472	28907	6.69	0.9280	39709	10.32
A3	0.9959	20020	3.40	0.9941	19299	3.62	0.4764	15638	2.31	0.8558	26722	6.13
n=3	0.9587	142610	43.49	0.9271	137189	41.29	0.9721	176374	53.85	0.9361	181282	54.51
Power 2	0.9610	21934	3.81	0.9875	21418	4.09	0.1551	−13569	−6.93	0.0009	−729	−2.34
$n = 2$	0.9858	104217	30.91	0.9659	100817	29.65	0.9871	122544	36.58	0.9632	129976	38.43
$n = 1.5$, $m = 0.5$	0.9841	48850	13.94	0.9615	47071	13.61	0.9744	67177	19.67	0.9523	76230	22.47
$n = 2.9$, $m = 0.1$	0.9557	130403	39.76	0.9230	125350	37.77	0.9708	165301	50.47	0.9335	170533	51.32
$n = 1.1$, $m = 0.1$	0.9400	4556	−0.34	0.8381	4074	0.00	0.8212	22883	6.15	0.8881	33234	9.70
$n = 1.9$, $m = 0.1$	0.9856	93143	27.53	0.9654	90067	26.45	0.9861	111470	33.20	0.9621	119227	35.24
$n = 2.3$, $m = 0.7$	0.9069	50526	15.30	0.8573	47999	14.72	0.9553	98860	30.18	0.9051	106038	32.16
$n = 1.5$	0.9951	87626	25.43	0.9836	85072	24.56	0.9829	95629	27.94	0.9772	104323	30.40
Model compensation	$a = -2.033\ \min^{-1}$, $b = 0.0003062\ \text{mol J}^{-1}$, $r^2 = 0.9906$			$a = -1.405\ \min^{-1}$, $b = 0.0002977\ \text{mol J}^{-1}$, $r^2 = 0.9896$			$a = -2.652\ \min^{-1}$, $b = 0.0003152\ \text{mol J}^{-1}$, $r^2 = 0.9939$			$a = -2.070\ \min^{-1}$, $b = 0.0003068\ \text{mol J}^{-1}$, $r^2 = 0.9929$		

[a] β (K/min).

obtained corresponds fairly well to the isoconversional activation energies, and the correlation coefficient is quite high, but better for the integral data than for the differential data.

The compensation effect in relation to the conversion was studied with the data obtained from the integral and differential isoconversional analysis, and was also based on a 0.1–0.9 conversion interval in steps of 0.01. Table 3 shows that the F1 model has a good correlation, with an isokinetic temperature of 133.2 °C for the integral data and 148.2 °C for the differential data. Both these temperatures fall within the experimental interval of temperatures and can therefore be accepted as valid. This criterion, however, cannot be used as a definite one, as there are more models with a temper-

Table 3
Compensation effect in relation to conversion, formulation 1:0

Model	Integral data			Differential data		
	$\ln k_{iso}$ ($\min^{-1}$)	T_{iso} (°C)	r^2	$\ln k_{iso}$ ($\min^{-1}$)	T_{iso} (°C)	r^2
D1	−3.326	113.6	0.9862	−0.563	156.5	0.9969
D2	−4.695	99.9	0.9810	−1.712	142.7	0.9956
D3	−7.140	83.1	0.9749	−3.828	126.7	0.9941
D4	−6.506	94.2	0.9790	−3.431	137.0	0.9951
F1	−0.942	133.2	0.9995	−0.086	148.2	0.9993
R2	−0.883	150.5	0.9988	−0.183	165.6	0.9995
R3	−1.519	145.0	0.9992	−0.787	159.7	0.9995
A2	1.580	177.6	0.9832	0.630	168.7	0.9988
A3	2.421	194.6	0.9695	0.695	175.9	0.9979
$n = 3$	−5.628	53.5	0.9901	−2.471	90.4	0.9954
Power 2	2.245	196.7	0.9747	1.595	200.0	0.9968
$n = 2$	−2.987	93.7	0.9970	−1.279	117.2	0.9978
n=1.5, $m = 0.5$	1.250	152.2	0.9905	0.499	144.1	0.9993
$n = 2.9$, $m = 0.1$	−4.752	62.6	0.9936	−2.116	94.8	0.9962
$n = 1.1$, $m = 0.1$	5.696	214.4	0.9456	1.922	168.6	0.9976
$n = 1.9$, $m = 0.1$	−6.073	−10.5	0.5544	−0.923	122.3	0.9983
$n = 2.3$, $m = 0.7$	1.403	140.0	0.9860	0.018	123.8	0.9991
$n = 1.5$	−1.878	114.0	0.9989	−0.682	132.1	0.9986

Table 4
Calculation of error rate in the estimation of $\ln A_\alpha$, according to Eq. (23), for the integral and differential data of formulation 1:0

Model	Integral data		Differential data	
	5[a]	10[a]	5[a]	10[a]
D1	4.28	4.11	3.78	3.26
D2	6.49	6.32	5.32	4.80
D3	12.29	12.13	10.10	9.60
D4	13.03	12.87	11.09	10.60
F1	1.41	1.53	1.61	1.60
R2	2.68	2.51	4.19	3.68
R3	4.27	4.10	5.39	4.88
A2	2.80	2.80	2.29	1.86
A3	3.30	3.27	3.24	2.78
$n = 3$	5.58	5.77	6.81	7.39
Power 2	2.53	2.41	4.36	3.90
$n = 2$	3.31	3.50	3.61	4.17
$n = 1.5$ $m = 0.5$	6.72	6.90	4.22	4.46
$n = 2.9$, $m = 0.1$	6.02	6.21	6.85	7.43
$n = 1.1$, $m = 0.9$	14.29	14.48	4.93	5.05
$n = 1.9$, $m = 0.1$	3.84	4.02	3.66	4.21
$n = 2.3$, $m = 0.7$	10.42	10.60	7.13	7.70
$n = 1.5$	2.29	2.47	2.43	2.65

[a] β (K/min).

ature within the experimental limits and a high correlation coefficient.

As has been described in Section 3.2, the value of $\ln A_\alpha$ was estimated based on the compensation in relation to the kinetic model. The compensation parameters for each heating rate, both integral and differential, can be seen in Table 2. Table 4 shows the error rates of the different models calculated according to Eq. (23). As can be seen, the error rate for the 5 and 10 K/min heating rates is lower in the F1 model, for both the differential and the integral data.

Figs. 10 and 11 show the estimations of the pre-exponential factor and its calculation based on isoconversional data and a model for the integral and differential data, respectively. As can be observed, the estimations in both cases are very similar to the calculation based on the model, except for very high conversions for the differential data.

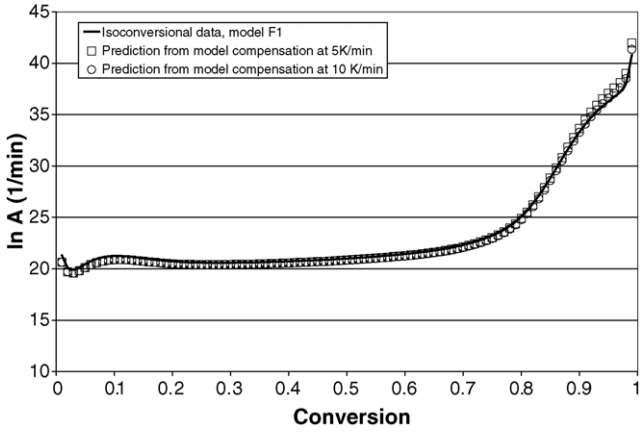

Fig. 10. Comparison between the predicted pre-exponential factor and applying the model, for formulation 1:0, integral data. The predictions made based on compensation in relation to the model and isoconversional activation energies appear as symbols. The unbroken line represents the calculation with the isoconversional data and applying the F1 model.

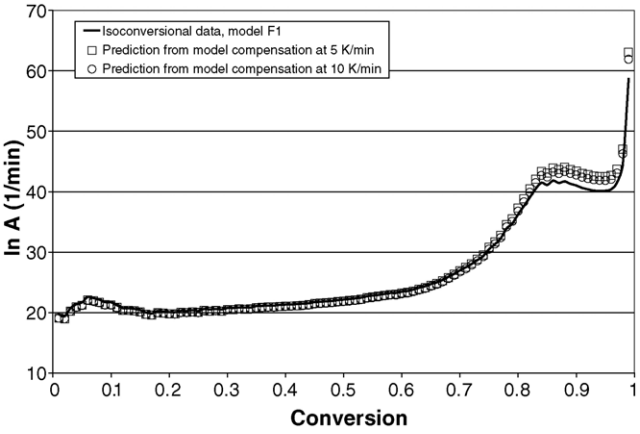

Fig. 11. Comparison between the predicted pre-exponential factor and applying the model, for formulation 1:0, differential data. The predictions made based on compensation in relation to the model and isoconversional activation energies appear as symbols. The unbroken line represents the calculation with the isoconversional data and applying the F1 model.

Given the good correspondence between the different methods applied, it can be stated that the F1 model is the one that best approximates to the curing of this formulation. A similar analysis was carried out on formulation 4:1, both for integral and differential data. The conclusion drawn is that the F1 model also properly approximates to the reaction process.

As the F1 model satisfactorily approaches to the reaction process, both in formulation 1:0, with ECH resin only, and in formulation 4:1, with an intermediate quantity of s(γ-BL), it is likewise assumed that it will be suitable for the other formulations as well.

The reaction rate is determined by the kinetic model $f(\alpha)$ and the kinetic constant, as can be seen in Eq. (5), where the kinetic constant k not only depends on the activation energy but also on the pre-exponential factor, according to the Arrhenius equation $\ln k = \ln A - E/RT$. As the activation energy and the pre-exponential factor may appear to be linked due to a compensation effect, a low energy value can be compensated by an equally low pre-exponential factor, and activation energy alone can not guarantee whether a system will be more or less reactive. The reactivity of the systems can be compared if the values of the kinetic constants are known. So, the pre-exponential factors must be calculated, and this can be done if a kinetic model that approximately describes the curing process has been previously established.

Table 5 shows the kinetic constant calculation, assuming that the F1 model is valid for calculating the pre-exponential factor, at a 0.5 conversion rate and a temperature of 100 °C. As can be seen, an increase in the proportion of s(γ-BL) increases the rate of reaction, both for integral and differential data, despite the fact that there is very little difference between

Table 5
Kinetic constants of the various formulations at 100 °C and 0.5 conversion rate, based on integral and differential isoconversional data, assuming that the F1 model is valid

Formulation	$\ln A_{0.5}$ (min^{-1})		$E_{0.5}$ (kJ/mol)		$k_{0.5,100\,°C}$ (min^{-1})	
	Differential	Integral	Differential	Integral	Differential	Integral
1:0	22.15	21.00	77.9	74.3	0.0528	0.0527
6:1	21.06	19.38	73.7	68.9	0.0682	0.0588
4:1	21.33	19.91	72.5	68.3	0.1304	0.1210
2:1	19.10	17.78	65.3	61.5	0.1429	0.1318
1:1	19.30	23.56	61.9	74.0	0.5209	0.7421

formulations 1:0 and 6:1, and between formulations 4:1 and 2:1.

5. Conclusions

It was seen that by adding s(γ-BL) to the ECH resin, the reaction process was speeded up and that it displaced curing at lower temperatures. Based on isoconversional data, it was seen that activation energy was generally diminished by adding s(γ-BL).

Several isoconversional methods were compared, both integral and differential, to obtain the activation energy for the entire reaction process. Vyazovkin's modified integral method gives, in the same way as Friedman's method does, the instantaneous and real value of activation energy at a given conversion rate, with a high degree of correspondence between the two methods.

The difference observed between the differential and integral methods is basically due to the different meaning of the activation energy in each of them. In order to analyze the processes that take place during curing, it is better to use differential data. However, for simulating isothermal or dynamic processes, or to determine the kinetic model, both integral and differential data can be used.

Based on the differential values of activation energy and the final peak observed in the dynamic thermograms, other relevant processes appear, which are associated with secondary reactions in ECH polymerized resin that appear at the end of the reaction process. The significance of these processes depends on the proportion of ECH in the formulations, being greater in formulations that are richer in ECH.

A high degree of correspondence was observed between the data obtained from FT-IR and simulations based on calorimetric data, assuming that the release of heat is a phenomenon mainly associated with the reaction of the epoxy groups in the various formulations, especially in the formulations with a higher ECH content.

By using the different methods available for determining the kinetic model, the model F1 was found to be the most suitable for the entire curing process. Kinetic constants were calculated assuming the model F1 is valid for the ECH/s(γ-BL) system, and an increase in reaction rate was observed as the s(γ-BL) content increased, which is in good agreement with the DSC reaction rate curves.

Acknowledgement

The authors would like to thank CICYT under Grant (MAT2004-04165-C02-02) for their financial support.

References

[1] X. Ramis, J.M. Salla, C. Mas, A. Mantecón, A. Serra, J. Appl. Polym. Sci. 92 (2004) 381–393.
[2] C. Mas, X. Ramis, J.M. Salla, A. Mantecón, A. Serra, J. Polym. Sci.: Part A: Polym. Chem. 41 (2003) 2794–2808.
[3] R.K. Sadhir, M.R. Luck (Eds.), Expanding Monomers: Synthesis, Characterization and Applications, CRC Press, Boca Raton, FL, 1992.
[4] L. Matejka, K. Dusek, P. Chabanne, J.P. Pascault, J. Polym. Sci.: Part A: Polym. Chem. 35 (1997) 665.
[5] C. Mas, A. Mantecón, A. Serra, X. Ramis, J.M. Salla, J. Polym. Sci.: Part A: Polym. Chem. 43 (2005) 2337–2347.
[6] C. Mas, A. Mantecón, A. Serra, X. Ramis, J.M. Salla, J. Polym. Sci.: Part A: Polym. Chem. 42 (2004) 3782–3791.
[7] X. Fernandez, J.M. Salla, A. Serra, A. Mantecón, X. Ramis, J. Polym. Sci.: Part A: Polym. Chem. 43 (2005) 3421–3432.
[8] H. Friedman, J. Polym. Sci. C 6 (1964–65) 183.
[9] D.C. Doyle, Nature 207 (1965) 240.
[10] T. Ozawa, Bull. Chem. Soc. Jpn. 38 (1965) 1881.
[11] P. Murray, J. White, Trans. Brot. Ceram. Soc. 54 (1955) 204.
[12] W. Coats, J.P. Redfern, Nature 207 (1964) 290.
[13] H.E. Kissinger, Anal. Chem. 29 (1957) 1702.
[14] T. Akahira, T. Sunose, Res. Report. Chiba. Inst. Technol. (Sci. Technol.) 16 (1971) 22.
[15] M.J. Starink, Thermochim. Acta 404 (2003) 163–176.
[16] G.I. Senum, R.T. Yang, J. Thermochim. Anal. 11 (1979) 445.
[17] P.K. Agrawal, Thermochim. Acta 297 (1997) 117.
[18] S. Vyazovkin, J. Comput. Chem. 18 (3) (1997) 393–402.
[19] S. Vyazovkin, D.J. Dollimore, Chem. Inf. Comput. Sci. 36 (1996) 42–45.
[20] J. Šesták, in: G. Svehla (Ed.), Thermophysical Properties of Solids. Their Measurements and Theoretical Thermal Analysis, Elsevier, 1984.
[21] S. Vyazovkin, Int. J. Chem. Kinet. 34 (7) (2002) 418–420.
[22] S. Vyazovkin, W. Linert, Chem. Phys. 193 (1995) 109–118.
[23] J.M. Salla, X. Ramis, J.M. Morancho, A. Cadenato, Therm. Acta 388 (2002) 355–370.
[24] J.M. Criado, Thermochim. Acta 24 (1978) 186.
[25] X. Ramis, J.M. Salla, A. Cadenato, J.M. Morancho, J. Therm. Anal. Cal. 72 (2003) 707–718.
[26] X. Ramis, A. Cadenato, J.M. Morancho, J.M. Salla, Polymer 44 (2003) 2067.
[27] L. Rong-Hsien, C. Chao-Lin, K. Li-Heng, Y. Ping-Rong, J. Appl. Polym. Sci. 82 (2001) 3539–3551.